The silicon lattice defects in proton and gamma irradiated n-channel CCDs

Conference or Workshop Item

Silicon lattice defects in proton and gamma irradiated n-channel CCDs.

Anton Lindley-DeCaire*, D. Hall, N. Bush, B. Dryer, A. Holland
Center for Electronic Imaging, The Open University, Milton Keynes, Mk7 6AA, UK

ABSTRACT

The Charge Coupled Device (CCD) has often been the imaging detector of choice for satellite missions. The space environments these camera systems operate in is abundant with highly energetic radiation. It is impossible to fully protect the CCD from the radiation environment, understanding the impact of radiation damage at a fundamental level is essential to characterise and correct the degradation on the image or spectrum. Here we study the properties of individual traps, with particular attention paid to the silicon divacancy, one of the major trap species found in n-channel CCDs caused by radiation damage that can effect image readout. Through the use of the trap pumping technique it is possible to observe individual traps and their properties in high detail with sub-pixel accuracy. Previous studies using the trap pumping technique have focused on proton irradiated CCDs to characterise the resulting defects. In addition to proton irradiated devices, the use of a ^{60}Co source allows the study of traps resulting from gamma irradiation and through this analysis a comparison can be made.

Keywords: CCD, divacancy, radiation damage, n-channel, image sensor.

1. INTRODUCTION

CCDs are widely used in space applications where radiation damage is one of the main challenges for space imaging. Missions such as Euclid[1], which will attempt to understand the nature of dark matter and dark energy, requires a level of accuracy of CCDs never before achieved in a space mission. To meet the targets of such future missions a fundamental understanding of the errors and damage mechanisms is needed. Radiation damage from energetic particles and gamma rays has the potential to displace a silicon atom from the silicon lattice, leaving a mobile vacancy defect and interstitial that can move through the lattice to find a stable structural pairing configurations; also called a trap. Depending on type of pairing, a trap can "steal" an electron from a charge cloud and reemit at a later time where the time is dependent on the said trap-types emission time-constant. The capture-reemission process leads to a signal that is smeared across the image. Over the lifetime of a space mission, radiation damage increases as it cannot be fully shielded against so even with optimisation of operating conditions and clocking schemes, the new defects need to be measured and accounted for during the mission.

The target of the study was to investigate differences between the impacts of different radiation types on the trap landscape of one of the major trap species, the silicon divacancy[2]. The method used to analyse the trap landscapes is the trap pumping technique that probes each pixel for a trap and measure properties such as the emission time constant of the trap, sub-pixel trap locations, probability of emission and energy levels. The temperatures probed range from 149 to 166 K, which covers acceptable parameter space of the double acceptor state of the silicon divacancy when probed using the trap-pumping technique.

2. RADIATION DAMAGE AND LATTICE DEFECTS

The radiation environment of space can be very harsh for silicon based detectors, with many species of highly energetic particles capable of damaging the detectors through ionisation effects and/or displacements of atoms from the detector lattice sites.

Sufficiently high energy radiation can displace an atom away from the regular crystalline structure position, potentially displacing the silicon atom into an irregular position in the lattice as an intrinsic interstitial atom and leaving a vacancy in the atoms previous location and warping the regular diamond structure of silicon into a more disordered structure.

Vacancies are capable of diffusion through the lattice over time to find stable configurations through combination with other lattice defects. Of the many potential defect combinations formed from the vacancy some are electrically active and create allowed energies in the bandgap that can capture an electron. One of the stable vacancy pairings that is highly abundant in irradiated devices is the double acceptor divacancy (VV or V_2^{--}). This double acceptor divacancy is found in the literature to have an energy level in the ranging from E_c = 0.225 to 0.23 eV [2,3] and has been found to be one of the four most abundant defect species found in irradiated CCDs[4].

There are two non-ionising types of radiation damage we are interested in comparing; point defects and clusters of defects. Point defects are predicted in proton irradiations below 10 MeV[5] where Coulomb scattering dominates and in ^{60}Co gamma rays. For protons between 6 to 10 MeV it has been suggested that a single defect cascade can occur with the ejected silicon energy between 1 to 2 keV, sufficient for small pairs of vacancies[6]. For proton energies greater than 10 MeV, nuclear scattering becomes non negligible and increase the number of cascading events that will cause clusters of defects. Clustering is expected to result in broader emission time constant peaks, the characteristic reemission time of a defect following capture of an electron/hole, due either to greater localised lattice damage or clustering distorting the emission time constant and energy levels.

The gamma spectrum of ^{60}Co has two significant energy peaks at 1.17 MeV and 1.33 MeV. If the higher energy gamma photons interact with an atom in the silicon lattice they have the potential to Compton scatter an electron at an energy greater than the 1 MeV threshold necessary for an electron to displace a single silicon atom in the lattice from an ejected electron. For proton energies below 10 MeV, the dominant displacement mechanism is the Coulomb interaction so in comparing the proton and gamma radiation sets we can measure any possible impact between point defects, single cascade and clustering on the distribution of energy levels for the defect energy levels and the trap landscape.

3. THE TRAP PUMPING TECHNIQUE

The goal of trap pumping is to probe the resonance of the emission time constant of the trap with the clock rate of the CCD. This is achieved by exposing the CCD to a flat field signal (10000 e^- is used for this paper) and moving the charge packet towards the readout and then return it backwards to the original location the trap that has captured an electron has the potential to release its charge into the nearest charge cloud; this can be the neighbouring charge cloud. The number of phases moved will differ device to device because of the number of phases in a pixel. A complete pump is when the charge cloud is moved forward and then brought back to its original position. This pump is repeated (10000 times for this analysis) until clear dipoles can be observed, as shown in Figure 1a. The process is then repeated across a range of phase times, the time held under one phase before moving the charge packet, until a full picture of efficiency of pumping is observed as shown in Figure 1b.

The charge capture and emission from a deep level traps and their energy levels can be well modelled by Shockley-Read-Hall (SRH) theory using two exponential time constants: the capture cross-section τ_c (Equation 1) and emission time constant τ_e (Equation 2)[7]. Terms for equations 1 and 2 are: n is the electron concentration, σ is the cross-section, $v_{th}$is the thermal velocity for electrons, N_c is the effective density of stated in the conduction band, E is the energy level of the trap, k is the Boltzmann constant and T is the temperature. An assumption is made that when the charge packet is over an empty electronically active trap that capture is 100% and instant because $\tau_c \ll \tau_e$.

The curve fitting method used a least-squares curve fit with Equation 3, where I is the amplitude of the dipole, N is the number of pumps, P_c is the probability of capture to account for a failure for 100% capture, t_{ph} is the unit of time between each charge packet transfer after the first phase when t = 0. The amplitude, I, of the dipole is found in this method by finding the difference between the brighter pixel that has received additional trap signal and the darker pixel that has donated/lost charge from the charge packet. Fitting SRH theory based equations to these curves determines the temperature specific emission time constant of the defect.

Energy levels are modelled by Equation 4 by least square fitting measured emission time constants across a range of temperatures: using the entropy factor X, field enhanced emission χ, the capture cross-section σ, thermal velocity v_{th} and density of states m_{dos}.

$$\tau_c = \frac{1}{n\sigma v_{th}} \quad (1)$$

$$\tau_e = \frac{1}{N_c \sigma v_{th}} \times \exp\left(\frac{E}{kT}\right) \quad (2)$$

$$I = NP_c\left(exp\left(\frac{-t_{ph}}{\tau_e}\right) - exp\left(\frac{-2t_{ph}}{\tau_e}\right)\right) \quad (3)$$

$$\tau_e = \frac{1}{X\chi\sigma N_c v_{th}} \exp\left(\frac{E}{kT}\right) \quad (4)$$

$$N_c = 2\left(\frac{2\pi m_{dos} kT}{h^2}\right)^{\frac{3}{2}} \quad (5)$$

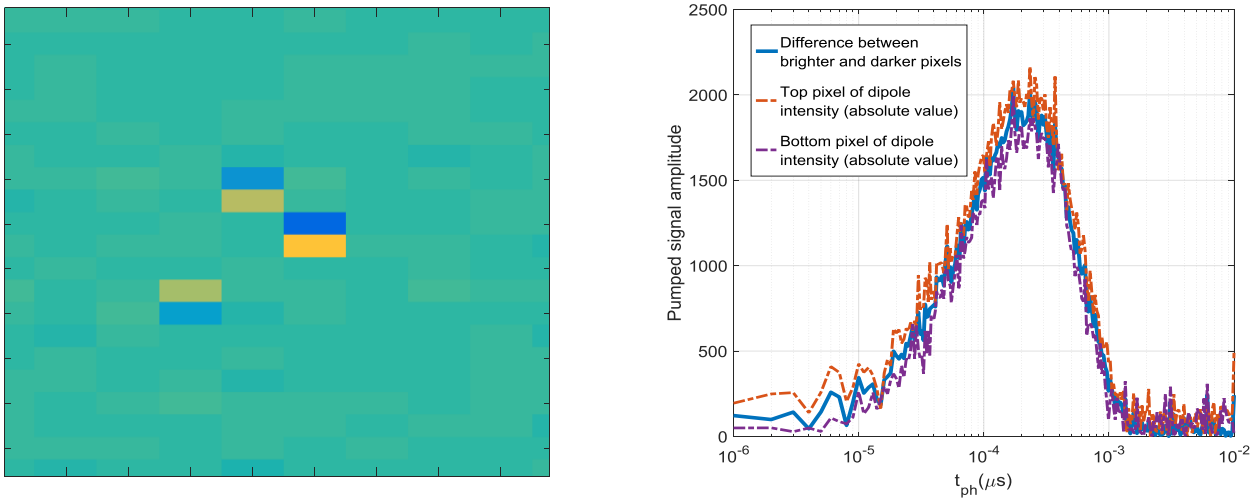

(a) Raw image dipoles following trap pumping

(b) Dipole intensity plot

Figure 1. (a) Small region of interest of raw trap pumping image showing a series of clear dipoles following 10000 pumps at a single pump time. (b) Shows overlaps of the dipoles top and bottom regions intensity of the trap following trap pumping through the range 10^{-6} to 10^{-2} μs. The difference between the two is the intensity profile that is curve fitted to determine if the dipole is caused by a trap.

4. EXPERIMENTAL TESTING

Two types of CCD were used in the study: for proton irradiations the AIMO CCD47-20s and for gamma irradiations the NIMO CCD347-20. The two devices have the same architecture however the AIMO device has implants to stop charge moving backwards. This limits trap pumping to one scheme as the method requires both forwards and backward shuffling of the charge packet. Only trap pumping in one scheme means only traps under certain electrodes can be probed but the impact on emission time constants, energy level and cross-sections will not be affected. The voltages necessary to run each device are different, most notably there is no substrate voltage applied to the gamma 347s and they are ultra-thin gate making them more resistant to ionisation damage. The trap pumping in done in a dark environment free of light producing noise sources so there should be minimal external signal. The CCD47-20s and the CCD347-20s have the same gate structures and can therefore use the same pumping schemes.

Table 1. Information on irradiation type, trap pumping temperature ranges

Device	Irradiation type		Trap pumping temperatures
	Radiation type	Dose	
CCD347-20 Device 1	None	None	154.70 to 155.16 K
CCD347-20 Device 2	^{60}Co Gamma	50 krad	156.75 to 160.38 K

CCD347-20 Device 3	^{60}Co Gamma	100 krad	149.37 to 153.96 K
CCD347-20 Device 6	^{60}Co Gamma	200 krad	150.42 to 161.99 K
CCD47-20 Device 2	6.5 MeV Proton beam line	6.74×10^9 protons/cm^2	154.38 to 162.16 K
CCD47-20 Device 4	72.8 MeV Proton beam line	2.53×10^{10} protons/cm^2	158.07 to 166.82 K

5. RESULTS AND DISCUSSION

5.1 Emission time constants

By trap pumping at temperatures ranging from 149 to 166 K, across pumping times from 1 μs to 10000 μs we can extract the emission time constant, cross section, and energy level of defects within this region of the parameter space for the divacancy, the less abundant stable traps and the continuum; the uncategorised stable traps that are found across the entire trap landscape[8].

Measuring the emission time constants from every successfully fitted dipole, we produce histograms of the emission time constants at a single temperature (155 K) for the CCD347-20 devices 1 (control) and device 6 (200 krad gamma), Figure 2. The vertical dashed lines show the range of emission time constants expected for the divacancy across the energy level range of 0.225 eV (left vertical dashed line) to 0.23 eV (right vertical dashed line), calculated from the recorded mean temperature of the trap pumping data which fluctuates in temperature during the complete sweep by less than ±0.1 K for all measurements shown. The trap present in the unirradiated CCD in peak 2 is predicted to be the C_iP_s III trap[9] with an equivalent energy level and cross-section of the divacancy that is not radiation induced so will not increase following irradiation[10].

Comparing the unirradiated device 1 with the gamma irradiated device 6 we can clearly see an increase in the number of divacancy traps (peak 2) whilst neighbouring traps continue to be present at an equivalent level (peak 3). Peaks 1 and 4 are statistical indicators to the number of traps that exist outside the measurement region. Peak 1 (10^{-6} s) is a successful fit to the tail of a trap that is too fast to observe the entire curve and peak 4 (10^{-2} s) is a successful fit to the beginning of another trap too slow to observe the entire curve; the emission time constants of these traps cannot be found within the temperature and emission time constant range covered here but are useful indicators of other radiation induced traps, showing that other species of trap than the divacancy are increasing in number following irradiation. The time parameter space probed is limited because faster readings cannot be achieved by the electronics and slower readings take a substantial amount of time.

The number of traps found across the predicted range of the divacancy in Figure 3 show the relative differences of different irradiation methods. Comparing the gamma irradiated devices 2 (50 krad) and 6 (200 krad), the number of traps under the divacancy peak increase by ~59% with a four-fold increase in the dose. There is the potential for divacancies to be hidden in the curves of different species which will be more numerous with the four-fold increase in radiation dose as well as effects such as CTI, bright pixels, dark current and pixel non-uniformity increases negatively impacting trap pumping.

For the proton irradiated devices the non-ionising energy loss (NIEL) hypothesis is used here to estimate and compare theoretical to experimental results of the displacement damage from different radiation types at different incident energies. Experimentally it is found that device 2, irradiated by 6.5 MeV protons has a ~57% increase in the number of traps under the major peak across the range of the divacancy than device 4, irradiated with 72.8 MeV protons. The theoretical and simulated model for NIEL predicts that at the fluences used for device 2, irradiated by 6.5 MeV protons has a NIEL dose of 1.62×10^{-4} MeV cm^2 g^{-1} Gy compared to device 4, irradiated by 72.8 MeV protons with a NIEL dose of ~$5.2e^{-5}$ MeV cm^2 g^{-1} Gy.

The emission time constant histogram of Figure 3 is normalised as shown in Figure 4. When comparing the two radiation damage types it is clear that gamma irradiated device have distinct delta-function time constants and proton irradiated do not with a tail of defects present. Proton irradiated devices 2 and 4 have equivalent full width half maximum (FWHM) and present similar tails of defects which are not observed for any fluence of gamma radiation.

The gamma irradiated devices should only exhibit point defects, whereas the proton irradiated devices, even at 6.5 MeV, exhibit clusters of defects causing nearby imperfections in the lattice structure to become more disorderly and distorting its properties in terms of the width of its energy level distribution and ability to capture charge[11,12].

The widths of the peaks are important to the operation of the CCD because we can optimise for minimum CTI by tuning the read out speed away from the major trap emission time constants; a narrow peak is therefore favourable as exhibited by the gamma irradiated devices, as this is easier to optimize away from. On the contrary a continuum of traps, as seen in the proton irradiated data as extended tails on the main peaks, is most difficult to determine an optimum clocking speed from knowledge of the trap landscape alone.

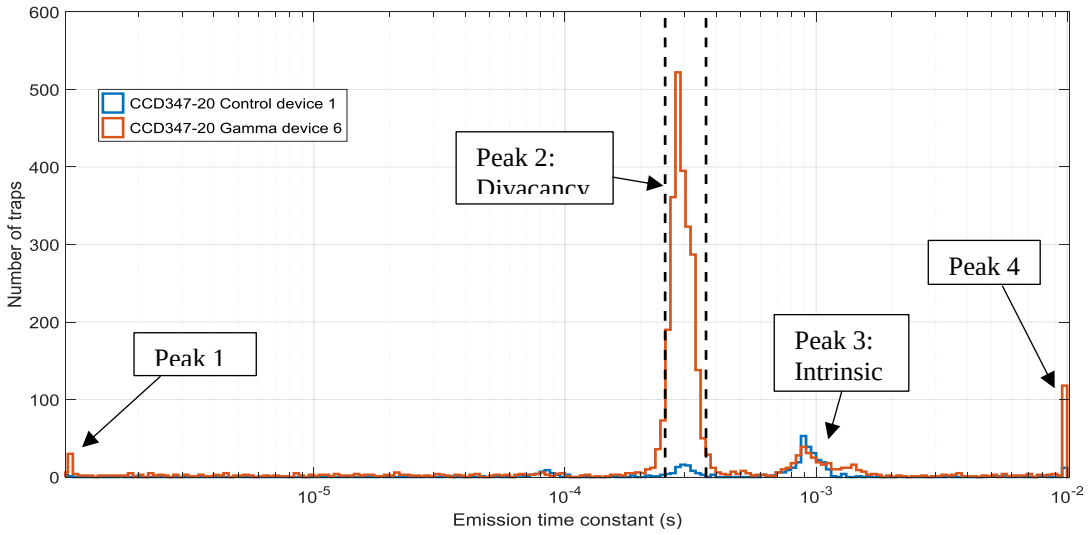

Figure 2. Comparison of emission time constant trap pumping histograms for CCD347-20 device 1 control (blue) and CCD347-20 device 2 gamma irradiated at 50 krad (orange); both at a temperature of 155 K. The black vertical lines are the theoretically modelled ranges of the emission time constants for the divacancy for 0.225 eV (left vertical line) and 0.23 eV (right vertical line).

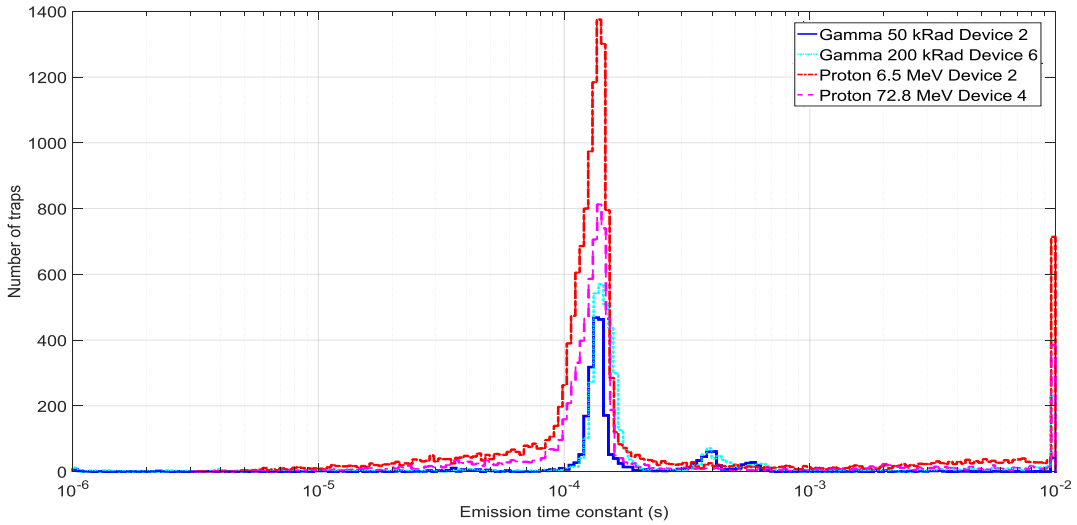

Figure 3. Comparison of proton low and high energy vs gamma for comparable emission time constants at equivalent temperature, 160 K.

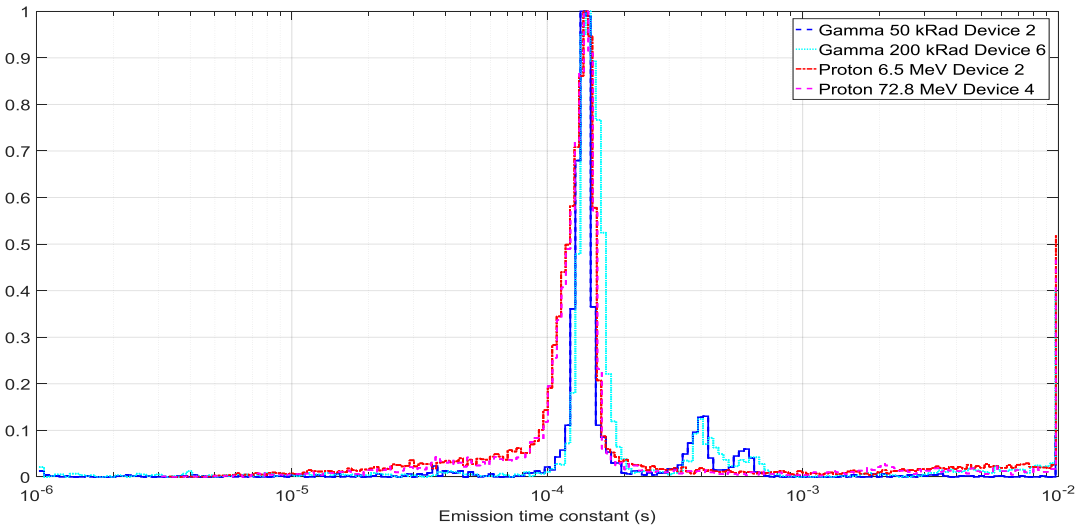

Figure 4. Emission time constant histogram, normalised and probed at equivalent temperatures, 160 K.

5.2 Energy level and cross-section

Studies of the silicon divacancy energy level are numerous[13,14,15] and indicate an energy level of Ec – (0.21-0.23) eV. Using the effective cross-section calculated[16,17] the energy levels of the peaks are confirmed to be in the range of the double acceptor divacancy, as shown in figure 5.

Table 2. Calculations of the energy level peak locations

	Gamma 100 krad	Gamma 200 krad	Proton 5.6 MeV	Proton 72.8 MeV
Energy level measured (eV)	0.230 ± 0.005	0.229 ± 0.005	0.231 ± 0.005	0.2275 ± 0.005

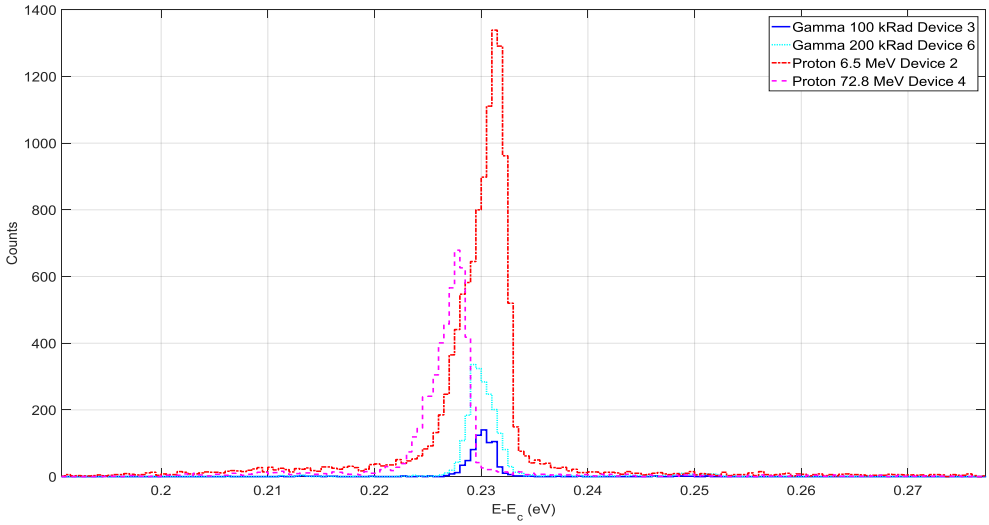

Figure 5. Energy levels histogram at a fixed effective cross-section of 1.3 x 10^{-15} cm^2.

6. CONCLUSIONS

We have presented a comparison of measured trap emission time constant landscapes for devices irradiated with both proton and gamma fluences, through the trap pumping technique. A difference between radiation types is presented here showing that proton irradiated devices form a large tail of defects from the divacancy that are not present in gamma irradiated devices. The results appear to indicate that at a certain NIEL threshold, radiation damage sources produce tails of defects that spread across the trap landscape and make CCD optimisation harder to achieve as fewer read out speeds can be chosen away from large trap concentrations.

The double acceptor level of the silicon divacancy energy level has been measured in agreement with the energy levels from DLTS studies, which range between 0.21 and 0.23 eV. The mean energy level was within error for each particle type, however the distribution of defects differed, potentially due to proton irradiated devices exhibiting clusters of defects as opposed to solely point defects in the gamma irradiated devices.

REFERENCES

[1] Laureijs, R. et al., "Euclid Definition Study Report," ArXiv e-prints, October 2011. http://arxiv.org/abs/1110.3193

[2] Corbett, J., "Silicon divacancy and its direct production by electron irradiation," Physical Review Letters, 7(8), 314-316 (1961).

[3] Moll, M., "Radiation Damage in Silicon Particle Detectors," Ph.D., University of Hamburg (1999).

[4] Bush, N., "The Impact of Radiation Damage on Electron Multiplying CCD Technology for the WFIRST Coronagraph," Ph.D., The Open University (2018).

[5] Zeigler, J. et al., "The stopping and range of ions in solids," Treatise on Heavy-Ion Science, 93-129 (1985).

[6] Wood, S. et al., "Simulation of Radiation Damage in Solids," IEEE Trans. Nucl. Sci., 28(6), 4107-4112 (1981).

[7] Hall, D. et al., "Determination of in situ trap properties in CCDs using a "single-trap pumping" technique," IEEE Trans. Nucl. Sci., 61(4), 1826-1833 (2014).

[8] Hall, D., "Mapping radiation-induced defects in CCDs through space and time," SPIE Proceedings: High Energy, Optical, and Infrared Detectors for Astronomy VII, 9915, (2016).

[9] Gürer, E. et al., "Configurational metastability of carbon-phosphorus pair defects in silicon," Materials Science Forum, 83, 339–344, (1992).

[10] Bush, N., "Development of in-situ trap characterisation techniques for EMCCDs," Journal of Instrumentation, 13(2), (2018).

[11] Svensson, B. et al., "Divacancy acceptor levels in ion-irradiated silicon," Phys. Rev. B, Condensed Matter, 43(3), 2292, (1991).

[12] Kuhnke, M., "Microscopic investigations on various silicon materials irradiated with different particles with the DLTS method," Ph.D., University of Hamburg (1999).

[13] Svensson, B., "Divacancy acceptor levels in ion-irradiated silicon," Phys. Rev. B 43, 2292, (1991)

[14] Brotherton, S., "Defect production and lifetime control in electron and γ-irradiated silicon," Journal of Applied Physics 53, 5720, (1982).

[15] Kimerling, L., "Defect States in Electron-Bombarded Silicon: Capacitance Transient Analyses," Radiation Effects in Semiconductors, Inst. Phys. Con, 31, 221-230, (1977).

[16] Hallén, A. et al., "Lifetime in proton irradiated silicon," Journal of Applied Physics, 79, 3906–3914, (1996).

[17] Wood, D. et al., "A study of the double-acceptor level of the silicon divacancy in a proton irradiated n-channel ccd", SPIE Proceedings: High Energy, Optical, and Infrared Detectors for Astronomy VII, 9915 (2016).